

REPORT NO. NADC-75324-30

7-8
- (P)



ULTRASONIC SPECTRUM ANALYSIS FOR NDT OF LAYERED COMPOSITE MATERIALS

W. R. Scott
Air Vehicle Technology Department
NAVAL AIR DEVELOPMENT CENTER
Warminster, Pennsylvania 18974

31 DECEMBER 1975

FINAL REPORT
AIRTASK NO. R02201001/DG204

D D C A
RECEIVED
AUG 26 1976
C
RW

APPROVED FOR PUBLIC RELEASE; DISTRIBUTION UNLIMITED

Prepared for
NAVAL AIR SYSTEMS COMMAND
Department of the Navy
Washington, D.C. 20361

ADA 028856

UNCLASSIFIED

SECURITY CLASSIFICATION OF THIS PAGE (When Data Entered)

9 Final rept.

| REPORT DOCUMENTATION PAGE | | READ INSTRUCTIONS BEFORE COMPLETING FORM |
|--|---|---|
| 1. REPORT NUMBER 17 NADC-75324-30 | 2. GOVT ACCESSION NO. | 3. RECIPIENT'S CATALOG NUMBER |
| 6 4. TITLE (and Subtitle) Ultrasonic Spectrum Analysis for NDT of Layered Composite Materials | 5. TYPE OF REPORT & PERIOD COVERED FINAL REPORT | |
| | 6. PERFORMING ORG. REPORT NUMBER | |
| 7. AUTHOR(s) 10 WILLIAM R. / SCOTT | 8. CONTRACT OR GRANT NUMBER(s) 11 31 Dec 75 | |
| 9. PERFORMING ORGANIZATION NAME AND ADDRESS NAVAL AIR DEVELOPMENT CENTER Air Vehicle Technology Department (Code 30) Warminster, Pennsylvania 18974 | 10. PROGRAM ELEMENT, PROJECT, TASK AREA & WORK UNIT NUMBERS AIRTASK NO. R02201001/DG204 | |
| 11. CONTROLLING OFFICE NAME AND ADDRESS Naval Air Systems Command Department of the Navy Washington, D. C. 20361 | 12. REPORT DATE 31 December 1975 | |
| | 13. NUMBER OF PAGES 36 (12) 40p. | |
| 14. MONITORING AGENCY NAME & ADDRESS (if different from Controlling Office) 16 NADC-FR-R022-01-001 | 15. SECURITY CLASS. (of this report) UNCLASSIFIED | |
| | 15a. DECLASSIFICATION/DOWNGRADING SCHEDULE | |
| 16. DISTRIBUTION STATEMENT (of this Report) Approved for public release; distribution unlimited. | | |
| 17. DISTRIBUTION STATEMENT (of the abstract entered in Block 20, if different from Report) | | |
| 18. SUPPLEMENTARY NOTES | | |
| 19. KEY WORDS (Continue on reverse side if necessary and identify by block number) Nondestructive Testing Ultrasonics Spectrum Analysis Laminates Composite Materials | | |
| 20. ABSTRACT (Continue on reverse side if necessary and identify by block number) The structural use of advanced composite materials has increased in recent years and a number of problems have arisen associated with assuring the integrity of composite structures. Because ultrasonics has emerged as an important tool for inspecting composite materials, it has become necessary to understand more about the interaction of acoustic waves with composites and what information can be obtained by monitoring this interaction. | | |

DD FORM 1 JAN 73 1473

EDITION OF 1 NOV 68 IS OBSOLETE
S/N 0102-014-6601

UNCLASSIFIED

SECURITY CLASSIFICATION OF THIS PAGE (When Data Entered)

407207

8

UNCLASSIFIED

SECURITY CLASSIFICATION OF THIS PAGE(When Data Entered)

In this paper a simple model is presented which predicts the ultrasonic frequency spectra for a broad class of layered composite materials having a finite number of laminae. Experimental verification of this model is demonstrated for arrays exhibiting both periodic and aperiodic frequency spectra. The relationship between the spectra of periodic arrays having both finite and infinite numbers of layers is discussed.

Important results relating to NDT which have emerged from this study include methods for predicting the results of spectrum analysis studies on layered materials and techniques for mapping small changes in the modulus and thickness of composite materials. Also discussed is the existence of forbidden frequency bands at which ultrasound cannot be transmitted through thick layered composites.



SECURITY CLASSIFICATION OF THIS PAGE(When Data Entered)

I N T R O D U C T I O N

A number of problems are associated with describing the propagation of ultrasonic waves in laminated materials. In general such materials are both inhomogeneous and anisotropic; therefore, there exist a number of modes of wave propagation associated with different directions of propagation. Attempts to treat these materials as monolithic materials with effective elastic moduli provide reasonable descriptions of quasi-static behavior;¹ however, when one attempts to describe transient phenomena with such a model, it is found that no choice of effective parameters is adequate to describe the high frequency behavior of propagating waves as influenced by the periodic nature of the composite. Recently a number of investigators^{2, 3} have approached the problem of waves propagating in a composite medium utilizing Floquet's Theorem for describing wave propagation in infinitely periodic structures. Most of this work on infinite laminates has been carried out in order to predict wave speeds associated with the effect of impact on laminates. These results have been promising; however, it is not clear to what extent they can be applied to finite periodic structures.

The problem of wave propagation in finite laminates has been considered by a number of investigators in the field of nondestructive testing,^{4, 5} who have been investigating the effect of laminates on the propagation of ultrasonic pulses, in order to develop nondestructive testing techniques for probing the structure of these laminates.

A number of investigators have observed periodic fluctuations in the frequency transmission and reflection spectra associated with laminated structures. This periodicity in the frequency spectrum has been explained⁶ as resulting from interference of coherent reflections of ultrasonic pulses from two separated interfaces within a sample.

It will be shown that this two interface model, while phenomenologically correct in some cases, fails in general to accurately describe wave propagation in laminates in which several interfaces exist. A modified model will be derived here which is capable of dealing with the general case of finite laminates and their ultrasonic frequency spectra. Also, the general interpretation of frequency spectra in laminates will be discussed with emphasis on applications of spectrum analysis to nondestructive testing of laminates and composites.

T A B L E O F C O N T E N T S

| | <u>Page No.</u> |
|--|-----------------|
| INTRODUCTION | 1 |
| LIST OF FIGURES. | 2 - 4 |
| THEORY | 5 |
| A. Acoustic Waves Incident on a Boundary. | 5 - 6 |
| B. Wave Propagation in a Single Layer | 6 - 7 |
| C. Attenuation in a Layer | 7 - 8 |
| E. Wave Propagation in Multi-Layered Media. | 8 - 9 |
| F. Calculations of Reflection and Transmission Spectra. . . | 9 |
| 1. Single Laminae in an Ambient Medium. | 9 |
| 2. Multi-Layered Periodic Media | 9 |
| 3. Infinite Periodic Media. | 10 |
| EXPERIMENT | 10 |
| RESULTS AND DISCUSSION | 11 |
| A. Transmission and Reflection Through a Single Finite Medium | 11 |
| B. Velocity of Sound Measurement. | 11 |
| C. Multilayer Media | 12 |
| D. Agreement between Theory and Experiment. | 12 |
| E. Frequency Spectra from Structural Composite Materials. . | 13 - 14 |
| F. Forbidden Frequency Bands in Composites. | 13 - 14 |
| G. Applications of Spectrum Analysis in Nondestructive Testing | 14 - 15 -16 |
| SUMMARY AND CONCLUSIONS. | 16 |
| RECOMMENDATIONS. | 17 |
| REFERENCES | 36 |

LIST OF FIGURES

| <u>Figure No.</u> | <u>Title</u> | <u>Page No.</u> |
|-------------------|--|-----------------|
| 1 | Ultrasonic Pulse Incident upon Medium of Finite Thickness | 18 |
| 2 | Ultrasonic Pulse Incident upon Layered Media | 19 |
| 3a | Transmission Spectrum for .30" Thick Steel Plate in Water | 20 |
| 3b | Reflection Spectrum for .30" Thick Steel Plate in Water | 21 |
| 3c | Transmission Spectrum for Glass Plate 1.22mm Thick in Water | 22 |
| 3d | Transmission Spectrum for two 1.22mm Glass Plates in Water | 23 |
| 3e | Transmission Spectrum for three 1.22mm Thick Glass Plates in Water | 24 |
| 3f | Transmission Spectrum for four 1.22mm Thick Glass Plates in Water | 25 |
| 3g | Transmission Spectrum for five 1.22mm Thick Glass Plates in Water | 26 |
| 4 | Apparatus for Measuring Acoustic Reflection and Transmission Coefficients as a Function of Frequency | 27 |
| 5 | Frequency Dependent Transmission of a .30" Steel Plate | 28 |
| 6 | Transmission Spectrum from Layered Array of three Glass Plates (Measured Experimentally) | 29 |
| 7 | Ultrasonic Frequency Spectra of Graphite Epoxy Panels | 30 |
| 8 | Ultrasonic Velocity vs Frequency in Graphite Epoxy | 31 |
| 9 | C-scan of Boron Aluminum Specimens | 32 |

L I S T O F F I G U R E S

| <u>Figure No.</u> | <u>Title</u> | <u>Page No.</u> |
|-------------------|---|-----------------|
| 10a | Ultrasonic Frequency Spectra for Boron Aluminum | 33 |
| 10b | Ultrasonic Frequency Spectrum for Boron Aluminum | 34 |
| 11 | C-scan for Graphite Epoxy Panel Showing Natural and Synthetic Flaws | 35 |

THEORY

A. Acoustic Waves Incident on a Boundary

It is a well known result⁷ that in the absence of dispersion the transmission and reflection amplitude coefficients T and R of acoustic plane waves incident normally from a medium with acoustic impedance Z_1 onto a medium of acoustic impedance Z_2 are given by:

$$(1a) R_{12} = \frac{Z_2 - Z_1}{Z_2 + Z_1} \quad (1b) T_{12} = \frac{2Z_2}{Z_2 + Z_1}$$

where the frequency independent Z for each medium is given by the product of the density ρ and the speed of sound C.

When more than two media are involved, interference effects produce frequency dependent transmission and reflection coefficients for waves traveling through media of finite thickness.

In general, for a given frequency, steady state solutions exist which can satisfy the boundary conditions for wave propagation through arbitrary laminar media; these solutions may be obtained through the solution of $2n-1$ linear simultaneous equations. The result of solving these equations is to generate steady state frequency dependent transmission and reflection coefficients. $T(\omega)$ and $R(\omega)$.

Because of the linear nature of the governing equations, implicit solutions to transient problems can be constructed from these transmission and reflection coefficients using a Fourier integral technique. For example if a number of layered media are impacted by a finite wave train of amplitude $A(t)$ and Fourier transform $A(\omega)$, the transmitted frequency and time dependent wave forms will be given by:

$$A_T(t) = \int e^{-i\omega t} T(\omega) A(\omega) d\omega$$

$$A_T(\omega) = T(\omega) A(\omega)$$

and the spectrum $A_{t_1 t_2}(\omega)$ of any time slice $(t_2 - t_1)$ of that transmitted wave train is given by:

$$A_{t_1 t_2}(\omega) = (2\pi)^{-\frac{1}{2}} \int_{t_2}^{t_1} A_T(t') e^{-i\omega t'} dt' \quad \left| \begin{array}{l} t_2 > t_1 > t=0 \end{array} \right.$$

where $t = 0$ is the time of arrival of the wave train at the first interface.

Both $A_{t_1 t_2}(\omega)$ (the spectrum of the total transmitted wave form) and $A_{t_1 t_2}(\omega)^T$ (the spectrum of the gated wave form), can be experimentally determined from ultrasonic measurements.

In this paper we will develop expressions for the quantities $T(\omega)$ and $R(\omega)$ by directly applying the principle of superposition to determine the response of a layered medium to a transient wave train.

This approach will generate a summable infinite series for $R(\omega)$ and $T(\omega)$; in addition to expressions for $A_{t_1 t_2}(\omega)$ from finite partial sums. An iteration scheme will be developed for calculating exact values of $R(\omega)$ and $T(\omega)$ for layered media. These values will be built up from the results for a single layer, and each successive iteration will add an additional layer to the medium. Thus in computing $T(\omega)$ and $R(\omega)$ for n layered media, results for $n-1$, $n-2$, $n-3$, etc. layers will be simultaneously generated.

B. Wave Propagation in a Single Layer

Consider the geometry of Figure 1. Let waves incident from the left upon medium 2 have transmission and reflection coefficients T_{12} and R_{12} and those incident from the right T_{21} and R_{21} . The coefficients for the boundary between medium 2 and 3 are analogously defined.

A portion of the pulse $A(t)$ incident from the left onto medium 2 will be transmitted with amplitude T_{12} and, upon emerging in medium 3, will produce a disturbance of the form

$$T_{23} T_{12} A(t - \frac{d}{c})$$

In addition to the portion of the wave transmitted into medium 2, there will be a number of pulses emerging which have undergone multiple reflections within this medium. The total of all of these waves is given by:

$$A'_{13}(t) = T_{12} T_{23} \sum_{N=0}^{\infty} (R_{23} R_{21})^N A(t - \frac{(2N+1)d}{c})$$

where $c = c_2$

Similarly the total wave reflected back into medium 1 is given by:

$$R'_1(t) = R_{12} A(t) + T_{12} T_{21} R_{21}^{-1} \sum_{N=1}^{\infty} (R_{23} R_{21})^N A(t - \frac{2Nd}{c})$$

Taking the Fourier transforms of expressions (2) and (3) and utilizing the identity

$$\int f(t - \Delta t) e^{i\omega t} dt = e^{-i\omega \Delta t} \int f(t) e^{i\omega t} dt$$

we have:

$$(4) A'_{13}(\omega) = \left[T_{12} T_{23} e^{-i\omega d/c} \sum_{N=0}^{\infty} (R_{23} R_{21})^N e^{-2i\omega Nd/c} \right] A(\omega)$$

$$(5) R'_1(\omega) = (R_{12} + T_{12} T_{21} R_{23} e^{-2i\omega d/c} \sum_{N=0}^{\infty} (R_{23} R_{21})^N e^{-2i\omega Nd/c}) A(\omega)$$

where $A'_{13}(\omega)$ is the Fourier transform of $A_{13}(t)$, and $R'_1(\omega)$ is the Fourier transform of $R_1(t)$, etc.

The sum appearing in expressions 4 and 5 can be readily evaluated for N either finite or infinite allowing the definition of generalized frequency dependent reflection and transmission coefficients $r(\omega)$ and $t(\omega)$ for the layered medium. For N infinite we have the expression

$$(6) t(\omega) \stackrel{d}{=} \frac{A'_{13}(\omega)}{A(\omega)} = \frac{T_{12} T_{23} e^{-i\omega d/c}}{1 - R_{23} R_{21} e^{-2i\omega d/c}}$$

$$(7) r(\omega) \stackrel{d}{=} \frac{R'_1(\omega)}{A(\omega)} = \frac{T_{12} T_{21} R_{23} e^{-2i\omega d/c}}{1 - R_{23} R_{21} e^{-2i\omega d/c}} + R_{12}$$

C. Attenuation in a Layer

The use of complex notation allows attenuation effects to be introduced into equations (6) and (7). This is done most easily by allowing d to be complex.

$$\tilde{d} = d(1 - i\alpha)$$

where d is a real distance and α becomes a linear attenuation coefficient, corresponding to a wave whose amplitude is exponentially damped with distance.

D. Generalized Reflection and Transmission Coefficients

Clearly, for the case of layered media of finite thickness a single reflection coefficient does not exist for the time dependent representation of the wave $A(t)$; however, we can define operators \hat{R} and \hat{T} which when operating on $A(t)$ generate the expressions for the time dependent reflected and transmitted waves respectively. The appropriate definition for these operations is:

$$\begin{aligned}
 (8) \quad \hat{R} A(t) &= \mathcal{F}^{-1}(\hat{r}(\omega) \mathcal{F}(A(t'))) \\
 &= (2\pi)^{1/2} \int_{-\infty}^{\infty} (\hat{r}(\omega) \exp(-i\omega t) (2\pi)^{-1/2} \int_{-\infty}^{\infty} A(t') \exp(i\omega t') dt') d\omega \\
 (9) \quad \hat{T} A(t) &= \mathcal{F}^{-1}(\hat{t}(\omega) \mathcal{F}(A(t'))) \\
 &= (2\pi)^{1/2} \int_{-\infty}^{\infty} (\hat{t}(\omega) \exp(-i\omega t) (2\pi)^{-1/2} \int_{-\infty}^{\infty} A(t') \exp(i\omega t') dt') d\omega
 \end{aligned}$$

where \mathcal{F} and \mathcal{F}^{-1} are the Fourier transform and its inverse. The use of this operator notation permits a layer to be represented as a boundary or virtual interface having these operators as their reflection and transmission coefficients (see Figure 2).

E. Wave Propagation in Multi-Layered Media

Consider the layered media in Figure 2. This is essentially the same as Figure 1 except that the boundary between media 2 and 3 is now replaced by a boundary medium with transmission and reflection operators \hat{R}_{23} and \hat{T}_{23}

Rewriting expressions (2) and (3) in the form of a series and replacing T_{23} and R_{23} by operators we have,

$$(10) \quad A'_{13}(t) = T_{12} \hat{T}_{23} \sum_{N=0}^{\infty} (\hat{R}_{23} \hat{R}_{21})^N A(t - (2N+1)d/c).$$

$$(11) \quad R'_1 = R_{12} A(t) + T_{12} \hat{T}_{23} \hat{R}_{23} \sum_{N=0}^{\infty} (\hat{R}_{23} \hat{R}_{21})^N A(t - 2Nd/c)$$

It is readily verified by recourse to their definitions that the transmission and reflection operators commute and that the Fourier transform of a number of operators acting on a function is just the product of the corresponding frequency reflection and transmission coefficients times the Fourier transforms of the function.

$$\begin{aligned}
 \hat{T}_N \hat{R}_N A(t) &= \hat{R}_N \hat{T}_N A(t) \\
 \text{and } \mathcal{F}(\hat{R}_N \hat{T}_N A(t)) &= \hat{r}_N(\omega) \hat{t}_N(\omega) \mathcal{F}(A(t))
 \end{aligned}$$

Applying these results to take the transform of expression (10) and (11) we have,

$$(12) \quad \hat{T}'_{13}(\omega) = \hat{A}'_{13}(\omega) / \hat{A}(\omega) = T_{12} \hat{t}_N(\omega) \sum_{N=0}^{\infty} (\hat{r}_N(\omega) \hat{R}_{21})^N \exp(-i\omega(2N+1)d/c)$$

$$(13) \quad \hat{R}'_1(\omega) = \hat{R}_{12}(\omega) + T_{12} \hat{T}_{23} \hat{r}_N(\omega) \sum_{N=0}^{\infty} (\hat{r}_N(\omega) \hat{R}_{21})^N \exp(-2iN\omega d/c)$$

Again summing the series we have,

$$(12a) \quad T^i(\omega) = T_{12} t(\omega) e^{-i\omega d/c} \\ \frac{1 - r(\omega) R_{21} e^{-2i\omega d/c}}{1 - r(\omega) R_{21} e^{-2i\omega d/c}}$$

$$(13a) \quad R^i(\omega) = R_{12} + T_{12} T_{21} r(\omega) e^{-2i\omega d/c} \\ \frac{1 - r_1(\omega) R_{21} e^{-2i\omega d/c}}{1 - r_1(\omega) R_{21} e^{-2i\omega d/c}}$$

Successive application of these formulae yields a simple iterative procedure for tabulating transmission and reflection coefficients for media having an arbitrary number of layers of varying thickness and acoustic parameters.

Normal incidence reflection and transmission coefficients for several finite arrays have been calculated using formulae (1a), (1b), (12a) and (12b) and the results of these calculations are discussed below.

F. Calculations of Reflection and Transmission Spectra

1. Single Laminae in an Ambient Medium

The values of the functions $\log_{10} |t(\omega)|$ and $\log_{10} |r(\omega)|$ for a 0.30" steel plate in water are plotted in Figures 3a and 3b respectively. The values of these coefficients were computed directly from expressions (12a) and (13a) using a Fortran computer program "Layer" written for this purpose. A computer controlled plotter was used to reproduce the plots directly from computed values with a resolution of 100 points per inch on the frequency axis. This resolution, although acceptable for plotting $\log_{10} |t(\omega)|$ is inadequate to reveal the sharp resonances in the function $\log_{10} |r(\omega)|$ which is in fact periodic. The existence of these sharp periodically spaced resonances termed thickness resonances (period $f = c/2d$) can be exploited for highly accurate sound velocity measurements.

2. Multi-layered Periodic Media

In addition to reproducing the known analytical results for transmission and reflection from single layers, "LAYER" has been applied to calculating $\log_{10} |t(\omega)|$ and $\log_{10} |r(\omega)|$ for finite periodic layered arrays. The results of such calculations are seen in Figures 3c through 3g, which plot $\log_{10} |t(\omega)|$ for stacks consisting of 1 to 5 glass plates 1.22mm thick spaced .1mm apart in an ambient medium of water. It is interesting to note that when more than a single plate is present $\log_{10} |t(\omega)|$ is no longer a simply periodic function.

The shallow tightly spaced minima seen in Figures 3d through 3g correspond roughly to the thickness resonance of the entire array and they increase in number as plates are added to the array. However, the broader resonances remain constant in number but rapidly deepen as layers are added, producing frequency bands having increasingly high acoustic attenuation.

3. Infinite Periodic Media

It can be shown that in the limit of a periodic medium with an infinite number of layers, there will be frequencies for which no traveling plane wave solutions exist inside the medium. This is a limiting case of the behavior seen in the transmission curves in Figures 3c through 3g. Robinson and Leppelmeier (Journal Applied Mechanics, March 1974, p. 89) have studied the case of wave propagation in a two component layered periodic medium and have given an expression for the wave number k of longitudinal traveling waves propagating in such a medium:

$$(14) \quad \cos kl = \cos \left(\frac{\omega d_1}{c_1} \right) \cos \left(\frac{\omega d_2}{c_2} \right) - \frac{1}{2} \left(\frac{\rho_1 c_1 + \rho_2 c_2}{\rho_2 c_2} \right) \frac{\sin \left(\frac{\omega d_1}{c_1} \right) \sin \left(\frac{\omega d_2}{c_2} \right)}{\rho_1 c_1}$$

where d_1 and d_2 are the layer thicknesses for media having sound velocities c_1 and c_2 respectively and $l = d_1 + d_2$. Whenever $\rho_1 c_1 \neq \rho_2 c_2$ in expression 14, there exist values of k for which $|\cos kl| > 1$. This implies a complex value of k and frequency regions corresponding to such wave numbers are referred to as forbidden bands, because there exist no traveling waves propagating at these frequencies. Using expression (14), the first four forbidden frequency bands have been calculated for the layered glass array of Figures 3c - 3g and are indicated by arrows in Figure 3g. It is seen that these forbidden bands correspond to broad transmission minima which are seen to deepen rapidly as the number of layers in the finite array is increased.

Experiment

Acoustic reflections and transmission coefficients were measured for a number of materials using the apparatus pictured schematically in Figure 4. Broadband longitudinal ultrasonic stress waves are projected onto a sample by a pulsed piezoelectric transducer (A). The projected pulse interacts with the sample producing transmitted and reflected wave trains. The transmitted wave train is detected by a second transducer (B) placed behind the specimen, while the reflected wave is detected by the projecting transducer.

Either the transmitted or the reflected pulse may be selected for amplification and gated electronically to obtain the desired portion or time slice of the signal. This gated signal is processed by a spectrum analyzer, which generates a plot of the amplitude of the gated signal as a function of frequency. (i.e. $|A_{t1t2}(\omega)|$)

RESULTS AND DISCUSSION

A. Transmission and Reflection Through a Single Finite Medium

Figure 5 shows the results of an experimental measurement of the frequency dependent transmission coefficient, $t(\omega)$, for a 0.30" steel plate. The projecting transducer in this measurement was a Panametrics VIP 15 MHz broadband device with a 1/4" diameter piezoelectric element; the receiver was a 25 MHz Automation Industries transducer with a 1/2" diameter element. The distance between the sample and the receiving transducer was 2". The gate was set to receive all of the transmitted pulse for which the amplitude was greater than the ambient noise.

The upper reference curve in Figure 5 is a plot of the logarithm base 10 of the amplitude of the signal produced at the receiving transducer vs. frequency (with no sample present). The lower curve is a plot of the logarithm of the transmitted amplitude as a function of frequency. The spectrum has a bandwidth of 1 KHz filtered to remove most of the rapid oscillations associated with the pulse repetition rate of the pulser receiver. Using this type of plot, the logarithm of the transmission coefficient can be measured as the difference in the ordinates of the two curves.

B. Velocity of Sound Measurement

The theoretical values for the transmission coefficient of a 0.3" steel plate computed from the absolute value of expression (6) are plotted in Figure 3a. The function is periodic with period

$$(15a) \quad \Delta f_N = \frac{c}{2d}$$

Frequencies for which (15a) is satisfied are often referred to as thickness resonances. Knowing the thickness of the plate this formula can be used to measure the phase velocity of sound as a function of frequency from experimental data using the relationship.

$$(15b) \quad c_{fN} = \frac{2fd}{N}$$

For steel this is most accurately measured using reflectance minima for which the resonances are much sharper than for transmission peaks (see Figure 5). The precision of this technique is easily better than one part in 1000 for steel; however, the variations in published values for c make it impossible to confirm these values to better than 2 significant figures.

C. Multilayer Media

Figure 6 is a plot of the transmission spectrum from a layered array of three glass plates .00122M thick separated by .001 meters of water. The entire array was immersed in water during the measurement and the system represents a somewhat idealized laminate. Figure 3e is a plot of the transmission spectrum for this laminate as computed from formulas 12a and 13a. The agreement between the theoretical and experimental spectra indicates that the linear acoustic approximation used is a reasonable model for wave propagation in laminated structures. Interesting features of the complicated laminate spectrum are:

1. Transmission peaks do not recur with simple periodicity as they do with monolithic materials.
2. Although peaks approximately corresponding to the first two thickness resonance modes for the entire array do appear, the third harmonic is absent and the next maximum appears after a large frequency gap.

These results are noteworthy because it has often been indicated in the nondestructive testing literature that reflections from a lamina-like structure within a specimen will produce a periodic spectrum. This is probably true only when other reflections in the structure are small, are of an essentially incoherent nature or can be isolated using a gating technique.

D. Agreement between Theory and Experiment

As mentioned above, velocities of sound measured by the spectrum analysis technique have been found to be in good agreement with published values. In addition, when published values for ρ and c are used in equations (1), (6) and (7) to compute spectra of laminates, we are able to compute positions and relative magnitudes of extremely detailed features of these spectra. (See Figures 6 and 3e).

A somewhat more conclusive test of the agreement between theory and experiment is the prediction and measurement of absolute values of transmission and reflection coefficients. For example, the minimum transmission coefficient of the steel layer in Figure 5 is about 4dB above its predicted value of -24dB and the maximum transmission coefficient, which should reach 0dB varies ± 2 dB from this value.

The observed discrepancy between theory and experiment is probably due to near field effects of the transducer. This hypothesis has been partially confirmed by experiments which have shown decreasing agreement between predicted and observed frequency spectra as frequency is increased. Since the near field of the transducer has a radius which is proportional to the transducer diameter divided by the square of the wavelength, the near field always extends further at high frequencies. Efforts to work entirely in the far field of the transducer have been hampered by poor signal to noise ratios and by the physical constraints of

the immersion tank. Improved agreement between theory and experiment may require the employment of analytical techniques for modeling near field transducer effects.

Additional experimental error results whenever the bandwidth of the spectrum analyzer is on the order of the spacing between spectral features. This results in the smearing out of sharp spectral features such as the transmission peaks in Figure 5, which should be much sharper and should reach a higher maximum value.

E. Frequency Spectra from Structural Composite Materials

Figure 7 shows a plot of the frequency spectra from three different graphite/epoxy laminates. For each of these spectra reflectance minima exist which correspond roughly to thickness resonances. (i.e. $f=Nc/2d$). This suggests that to a first approximation, a graphite epoxy laminate may be modeled as a monolithic material. However, it is seen that as in the case of the layered glass laminate the portion of the frequency spectrum corresponding to the thickness resonance of a single period of the laminate behaves anomalously (i.e. resonance number 4 is missing for the 4 ply laminate, resonance number 18 is missing for the 18 ply laminate). Pursuing the implications of modeling the composite as a monolithic material, formula (15b) may be applied to compute a dispersion relation $c(f)$ for each frequency at which a thickness resonance occurs. Such a dispersion relation is plotted in Figure 8 for an 18 ply graphite/epoxy laminate. Significant features of this dispersion relation are,

(1) A general increase in velocity with increasing frequency, (a phenomenon expected in viscoelastic materials).

(2) Finite discontinuities in velocity at multiples of 4 MHz.

F. Forbidden Frequency Bands in Composites

The existence of discontinuities in the dispersion relations for composite materials results from the periodic structure of the composite and may be predicted from equation (14) and the relation,

$$c=f/2\pi k$$

It is found that finite discontinuities in velocity occur when frequencies of high attenuation referred to as forbidden frequency bands are reached. Alternately we may say that these discontinuities occur whenever the wave number K is a multiple of $2\pi/l$ where l is the thickness of one period of the medium. (See Figure 7). Thus, although wave propagation does not cease in the forbidden bands for finite layered laminates, transmission is strongly attenuated. In addition if experimentally measured dispersion curves for finite media are examined, it is found that regions of anomalous dispersion occur in the vicinity of the forbidden bands.

It is interesting to note that the graphite/epoxy composites whose spectra are plotted in Figure 7 are not laid-up in a truly periodic array but consists of 0° , 90° and $\pm 45^\circ$ layers. Some indication of the effects of ply arrangement can be seen in Figure 7 (Velocity dispersion for an 18 ply composite). In addition to the discontinuities which occur near 8 and 16 MHz corresponding to resonances of a single layer, anomalies also occur near 4 and 12 MHz which correspond to resonances of lamina pairs. Strictly speaking one cannot explain such resonances in terms of the simple theory presented here, since for normal incidence longitudinal waves identical angle ply laminae of different orientation should behave identically. It appears that for the general graphite/epoxy laminate a detailed model for stress wave propagation must include the effects of waves being scattered in directions other than parallel to the incident wave.

G. Applications of Spectrum Analysis in Nondestructive Testing

The reasonable success in modelling the ultrasonic frequency spectrum of layered materials and the empirically confirmed capability of predicting qualitatively the frequency spectra of fiber reinforced composites suggest a number of nondestructive testing applications.

The existence of thickness resonances in the reflection and transmission spectra of composites, analogous to those present in monolithic materials, suggest that a type of generalized thickness gauging can be performed using spectrum analysis. For example the peak position of thickness resonances below the forbidden band may be given approximately by the expression,

$$(16) \quad f_{\text{peak}} = nc/2d \quad (\text{for } n \text{ less than the number of laminae})$$

where d is the thickness of the composite

n is an integer

and c is the phase velocity of sound in the composite.

Clearly, the position of the resonance peak is a function of the sample thickness and the velocity of sound, the latter being a function of the elastic constants (c_{ij}) of the material and its density.

For longitudinal waves propagating normal to the surface of a composite with hexagonal symmetry, the velocity of sound in the low frequency limit is given by,

$$c = c_{33}/\rho$$

Thus the resonance peak position in the composite spectrum can be used to monitor variations in density, thickness and elastic constants. An efficient means of accomplishing this monitoring is to use the amplitude of one component of the frequency spectrum at or near a resonance peak to modulate the intensity of a c-scan. In this manner a composite sample may be imaged using a particular frequency of ultrasound. For sharp resonances small changes in thickness or modulus will cause large changes in the amplitude of ultrasound being transmitted at or near this frequency, producing corresponding changes in c-scan intensity.

An example of such a transmission c-scan is shown in Figure 9, which is a c-scan of two boron/aluminum 4 ply unidirectional tensile specimens. The nominal thickness of these specimens is 0.041" and their ultrasonic thickness resonances for longitudinal waves occur at about 3.8 MHz. (see Figures 10a and 10b). The c-scan intensity was modulated using the amplitude of the spectral component centered at 3.7 MHz. In this manner slightly thicker specimens having peak transmission at lower frequencies produce darker c-scans than thinner ones. In fact, micrometer measurements of the specimens showed that the darker specimen (#1716 Figure 9) had an average thickness of 0.0419", while the lighter specimen had an average thickness of 0.0402". Ultrasonic frequency spectra plotted for selected positions on each specimen show that the expected resonance shifts do in fact occur, the frequency shift between the dark and light areas being about 0.2 MHz.

The agreement between these two results may be checked by differentiating formula (16) which gives for the frequency shift,

$$\Delta f_{\text{peak}} = -(\Delta d/d) \cdot f_{\text{peak}} = 0.19 \text{ MHz}$$

This result is well within the experimental variation in the thickness measurements.

In addition to the difference in average intensity observed between the two specimens in Figure 9 there is a variation seen within each specimen. This gradation in shading appears as bands oriented parallel to the fiber direction in the specimens. These bands also have frequency shifts associated with them, and the peak intensity of the spectral thickness resonances associated with the bands varies only slightly. This indicates that these bands are associated with thickness or modulus variations rather than delaminations.

The sensitivity of the resonances to delaminations can be seen in Figure 11, which is a c-scan of a graphite/epoxy panel for which the intensity is modulated by the acoustic amplitude corresponding to a reflection thickness resonance (antiresonance). This amplitude is small except in the presence of defects. Using this technique a number of natural and synthetic defects were revealed without the necessity of accessing both sides of the sample.

A potential application of the analytical model presented here is the prediction of the frequency spectra from diffusion bonded or adhesively bonded laminates with arbitrary stacking. Because the model is quite accurate for arrays of monolithic materials, the spectrum resulting from a particular condition in the laminate can be predicted without reference to standard specimens.

S U M M A R Y A N D C O N C L U S I O N S

A model has been constructed for describing the interactions of ultrasonic plane waves with laminated structures. Using this model measurable parameters such as the frequency dependent transmission and reflection coefficients can be accurately calculated for laminates consisting of layers of elastic monolithic materials.

Experiments and calculations for some simple finite periodic laminates have demonstrated the following:

(1) In general ultrasonic frequency spectra of laminates including periodic laminates are not simply periodic functions.

(2) If a finite periodic laminate is modeled using the model for an infinite laminate, regions of high frequency attenuation will be localized accurately for laminates having a sufficient number of layers. However, this model cannot predict detailed transmission or reflection spectra.

(3) For wavelengths longer than λ (where λ is the period of the laminate) periodic laminates behave acoustically in much the same way as dispersive monolithic materials and their transmission and frequency spectra exhibit thickness resonances, with spacing $\Delta f = \frac{c(f)}{2d}$, where $c(f)$ is the phase velocity in the composite. For wavelengths on the order of $n\lambda$ (n an integer) the laminate exhibits anomalous dispersion and strong attenuation.

(4) Structural composites (e.g. graphite/epoxy, fiberglass, B/Al) have acoustic properties which are qualitatively similar to those described above for simple laminates.

The characteristics of laminate spectra reveal a number of very important facts which should be considered when performing ultrasonic inspection of layered composite materials.

When inspecting thick laminates ultrasonically, the existence of forbidden transmission bands and narrow thickness resonances dictates that ultrasonic frequencies be carefully selected. This is particularly important if tuned transducers are being used. The location of forbidden frequency bands will vary with material properties, thickness, lay-up and the number of plies in a laminate but will remain relatively constant in thick laminates having the same periodicity.

Features of ultrasonic spectra can be used as sensitive monitors of changes in thickness and modulus both of which are linearly related to thickness resonance frequencies. Acoustic amplitudes of waves propagating near these resonant frequencies can be used to modulate c-scan intensities, thereby generating maps of a sample, which reveal small changes in either modulus or thickness.

The model which has been constructed for ultrasonic wave propagation in laminates has proven to be quite accurate in predicting detailed features of the ultrasonic frequency spectra of layered structures and should be useful for describing wave propagation in any structure consisting of monolithic laminae.

RECOMMENDATIONS

1. The existing model for wave propagation in laminates should be applied to more complicated laminates including laminates with defects and aperiodic arrays. This modeling will require the use of effective parameters when dealing with viscoelastic and fiber reinforced materials.
2. Efforts should be made to generalize the present model to cases involving scattering, shear wave propagation and propagation of waves at oblique incidence to laminate interfaces.
3. Ultrasonic NDT techniques and devices should be developed which exploit the resonant nature of laminated structures. These might include the following:
 - a. Selection of frequencies for maximum penetration into laminates.
 - b. The use of tuned transducers, filters and amplifiers for improved signal-to-noise ratio when interrogating laminated composites near their resonant frequencies.
 - c. The use of multi-frequency techniques for monitoring lay-ups and consistency in structural composites.

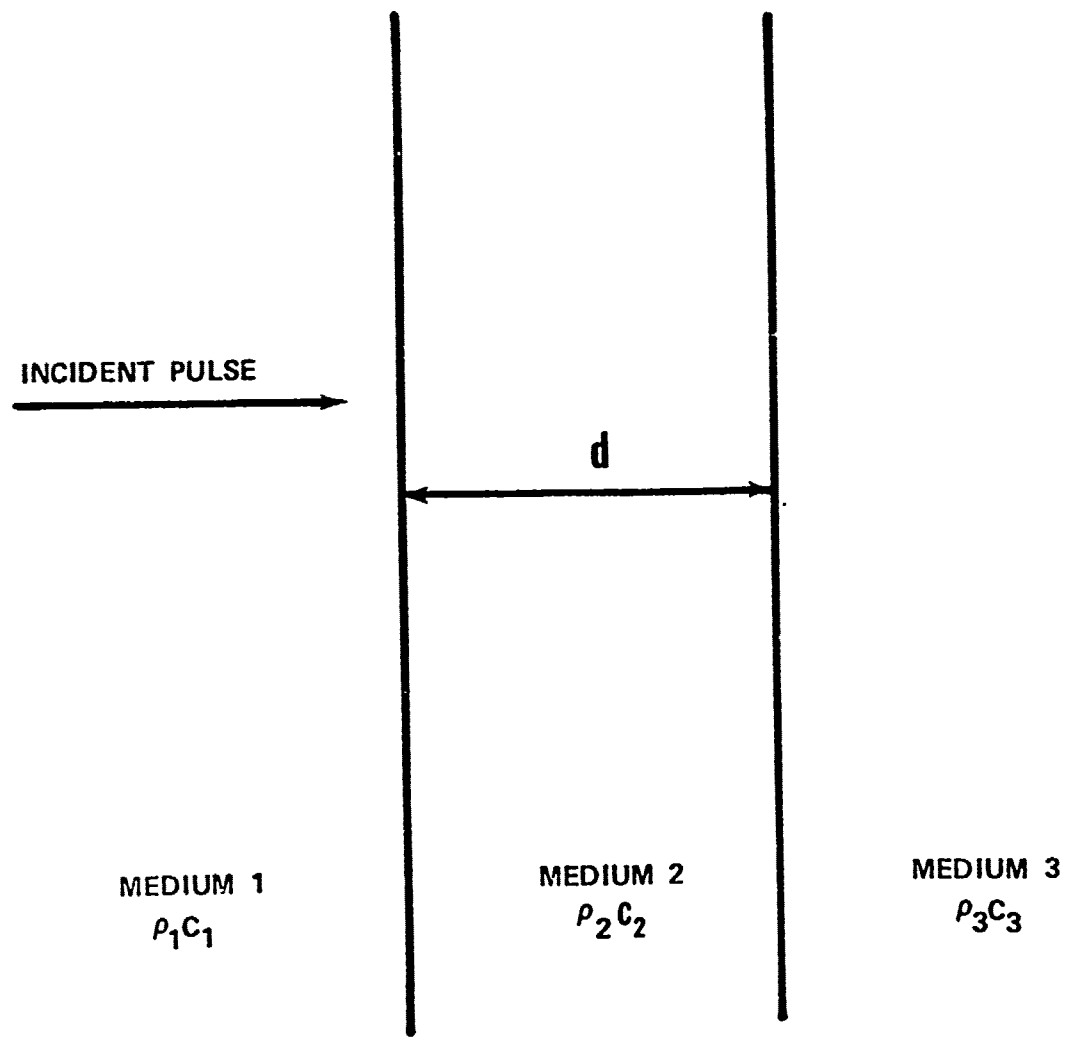


Figure 1 Ultrasonic Pulse Incident upon Medium of Finite Thickness

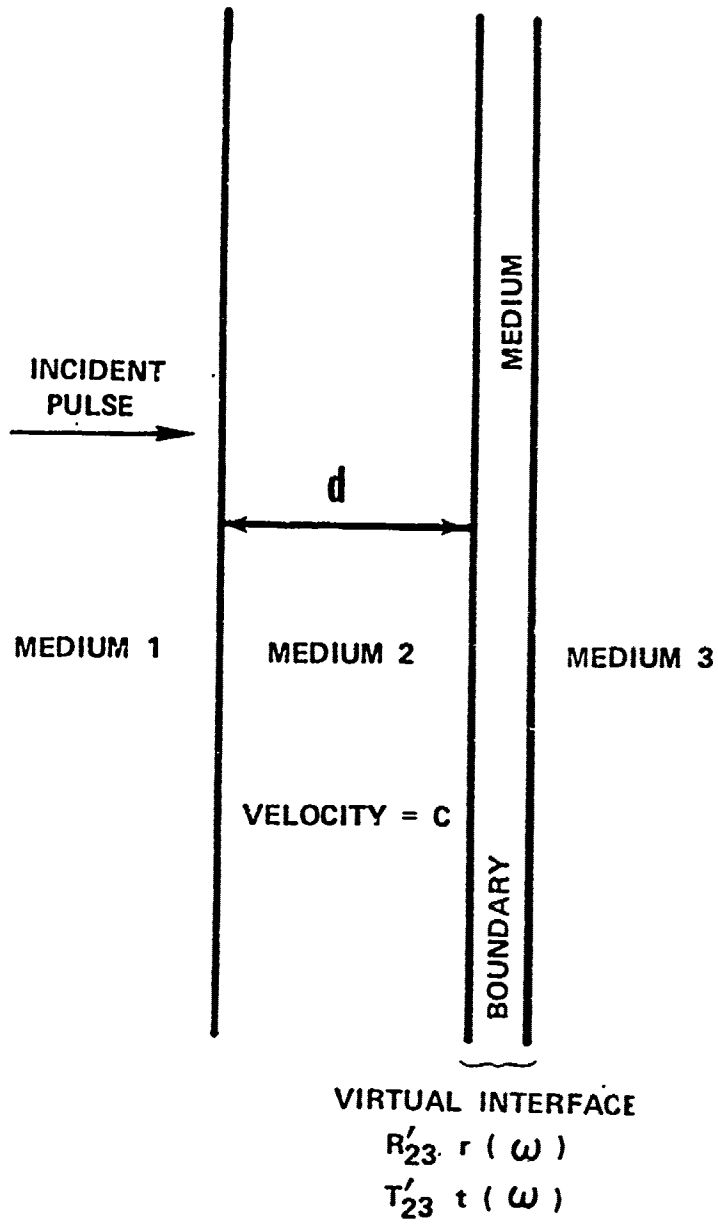


Figure 2 Ultrasonic Pulse Incident upon Layered Media

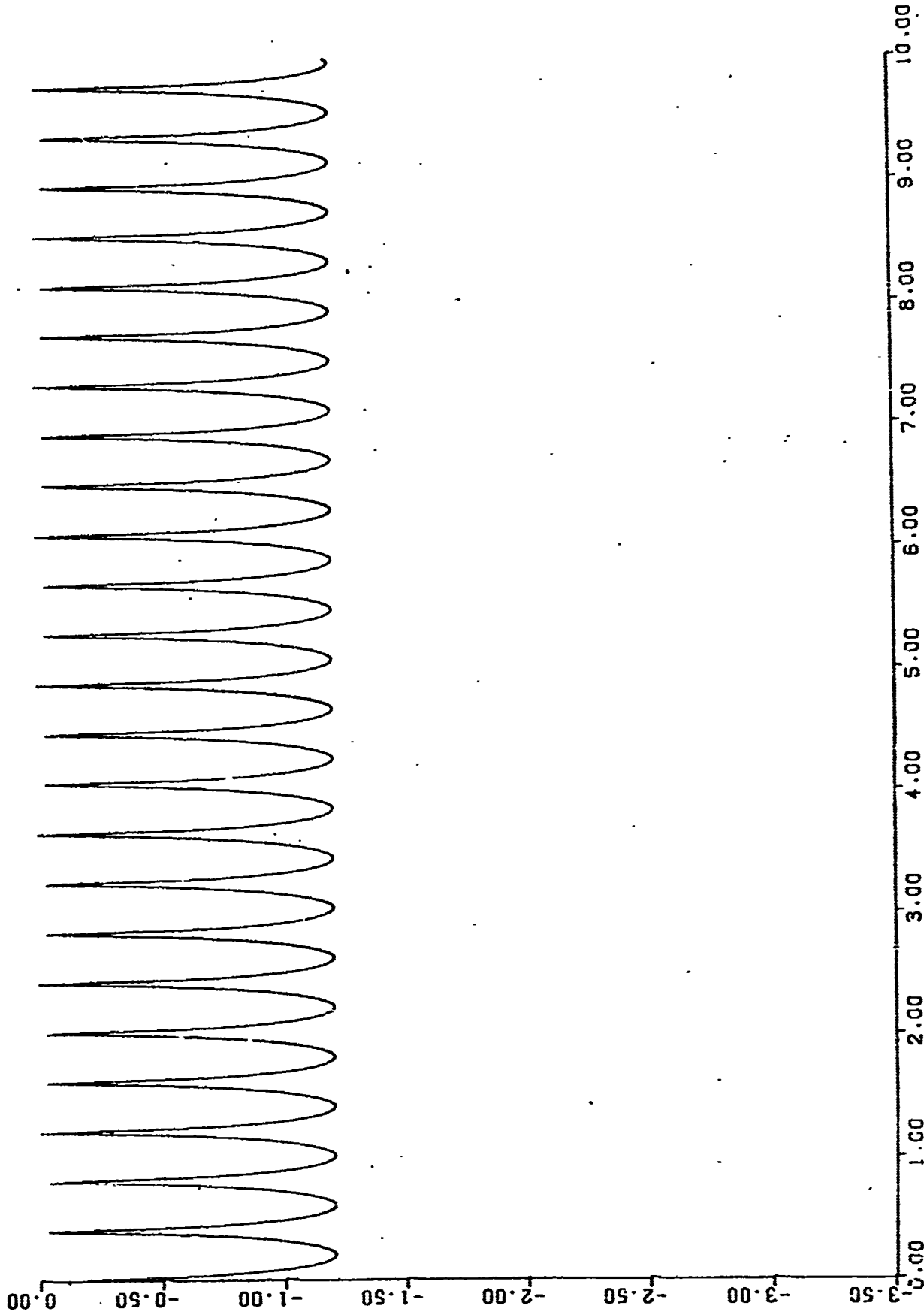


Figure 3a Transmission Spectrum for 0.30" Thick Steel Plate in Water

NADC-75324-30

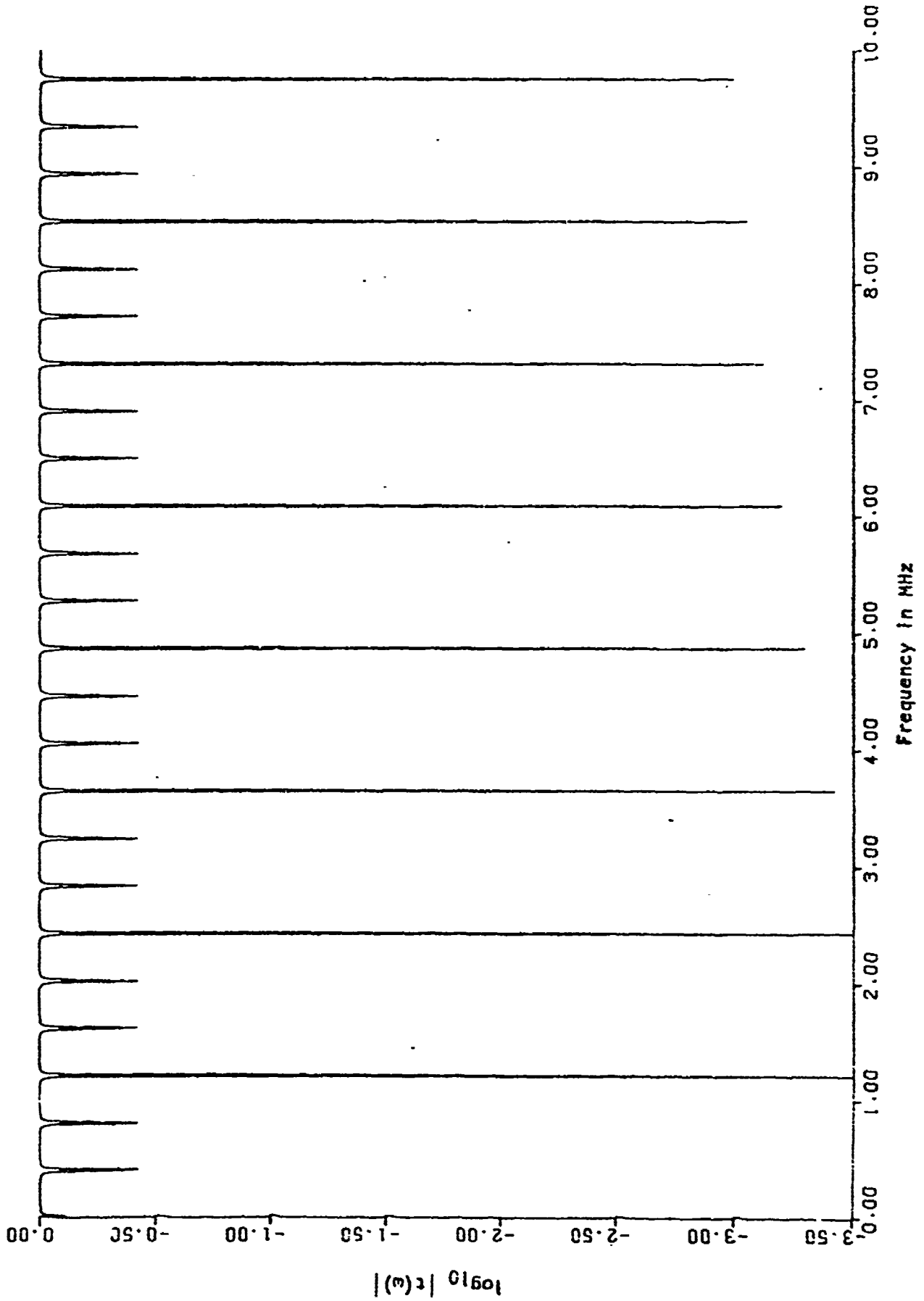


Figure 3b Reflection Spectrum for 0.30" Thick Steel Plate in Water

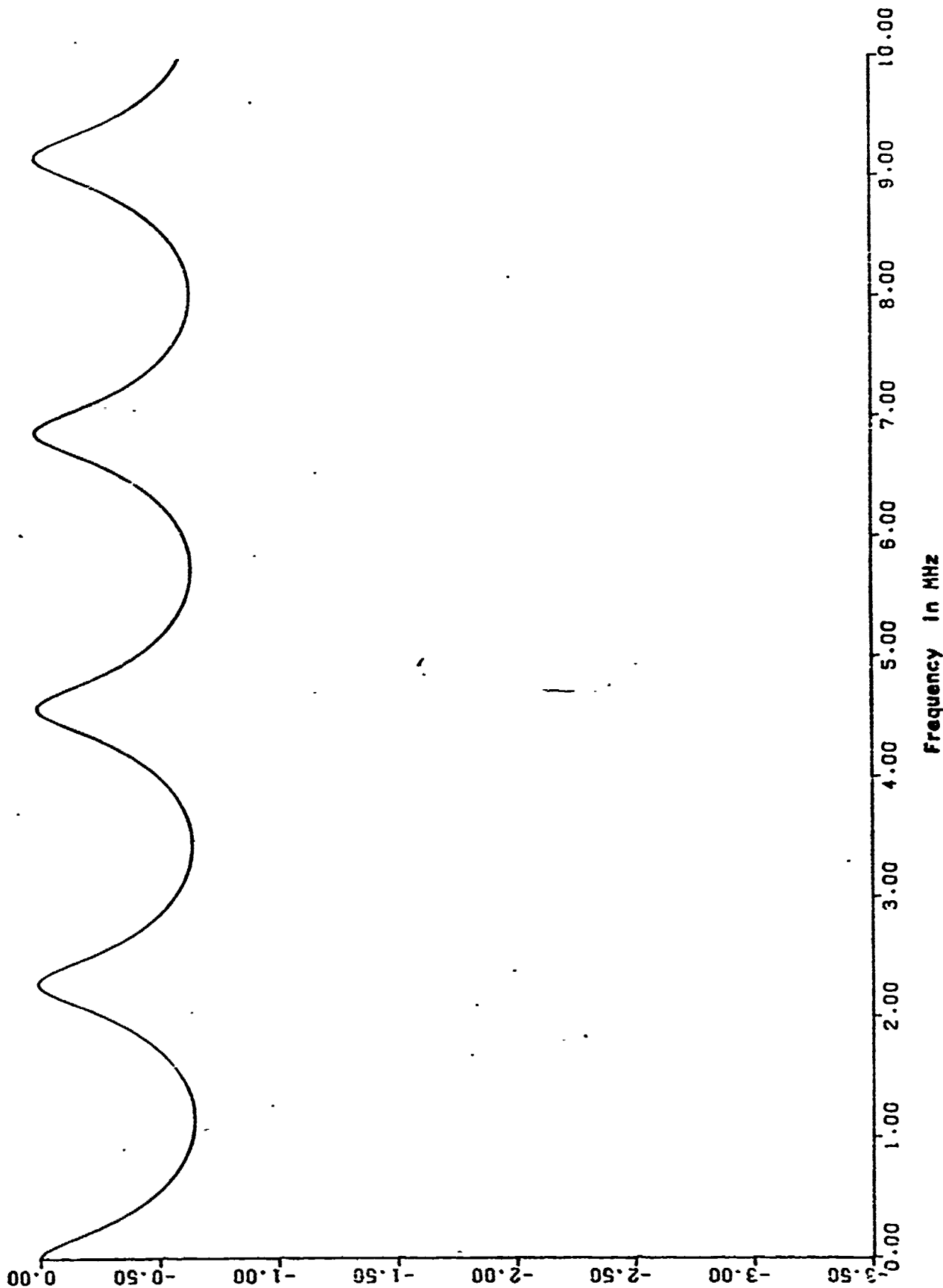


Figure 3c Transmission Spectrum for Glass Plate
1.22mm Thick in Water

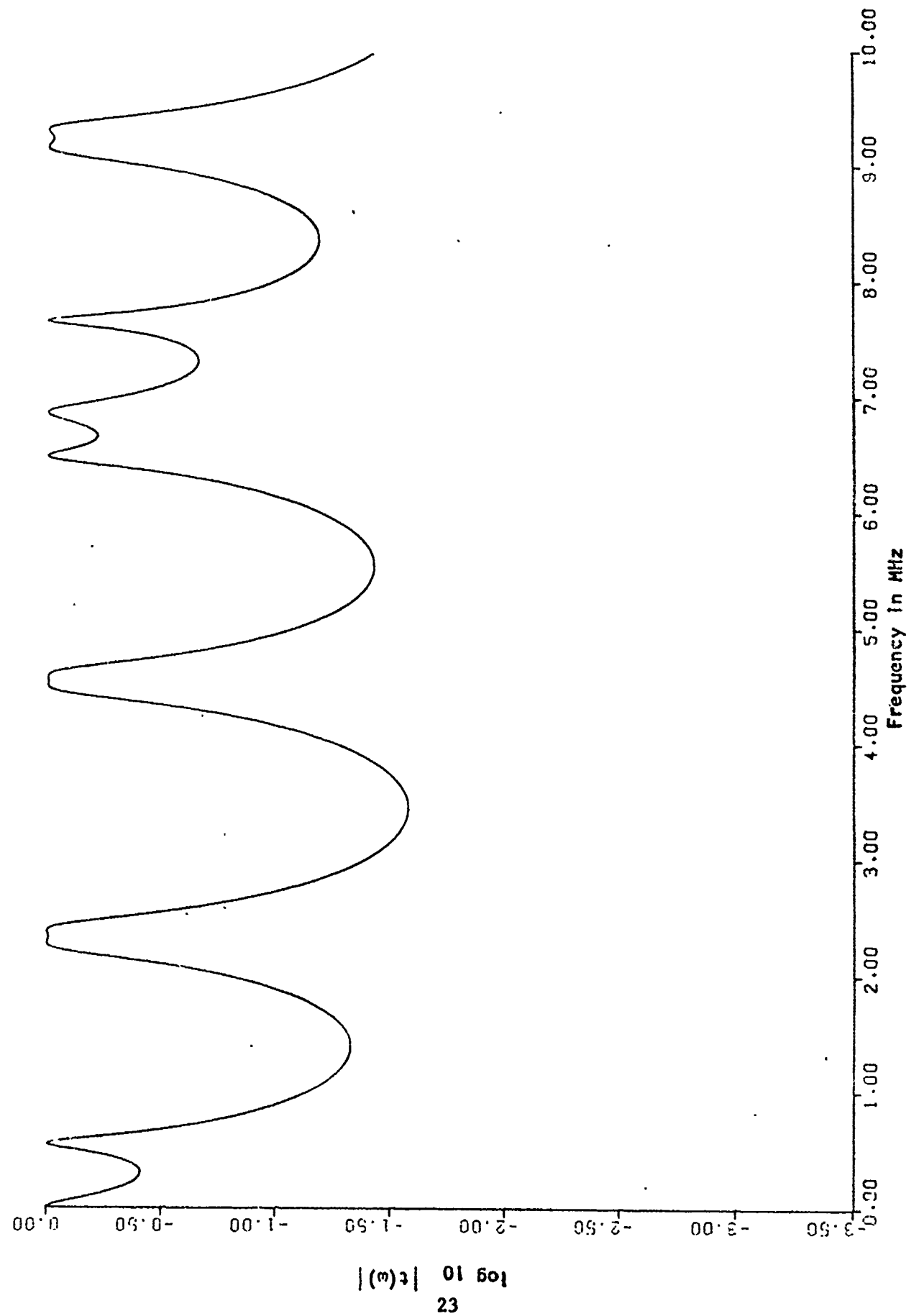


Figure 3d Transmission Spectrum for two 1.22mm Glass Plates in Water (0.1mm separation)

NADC-75324-30

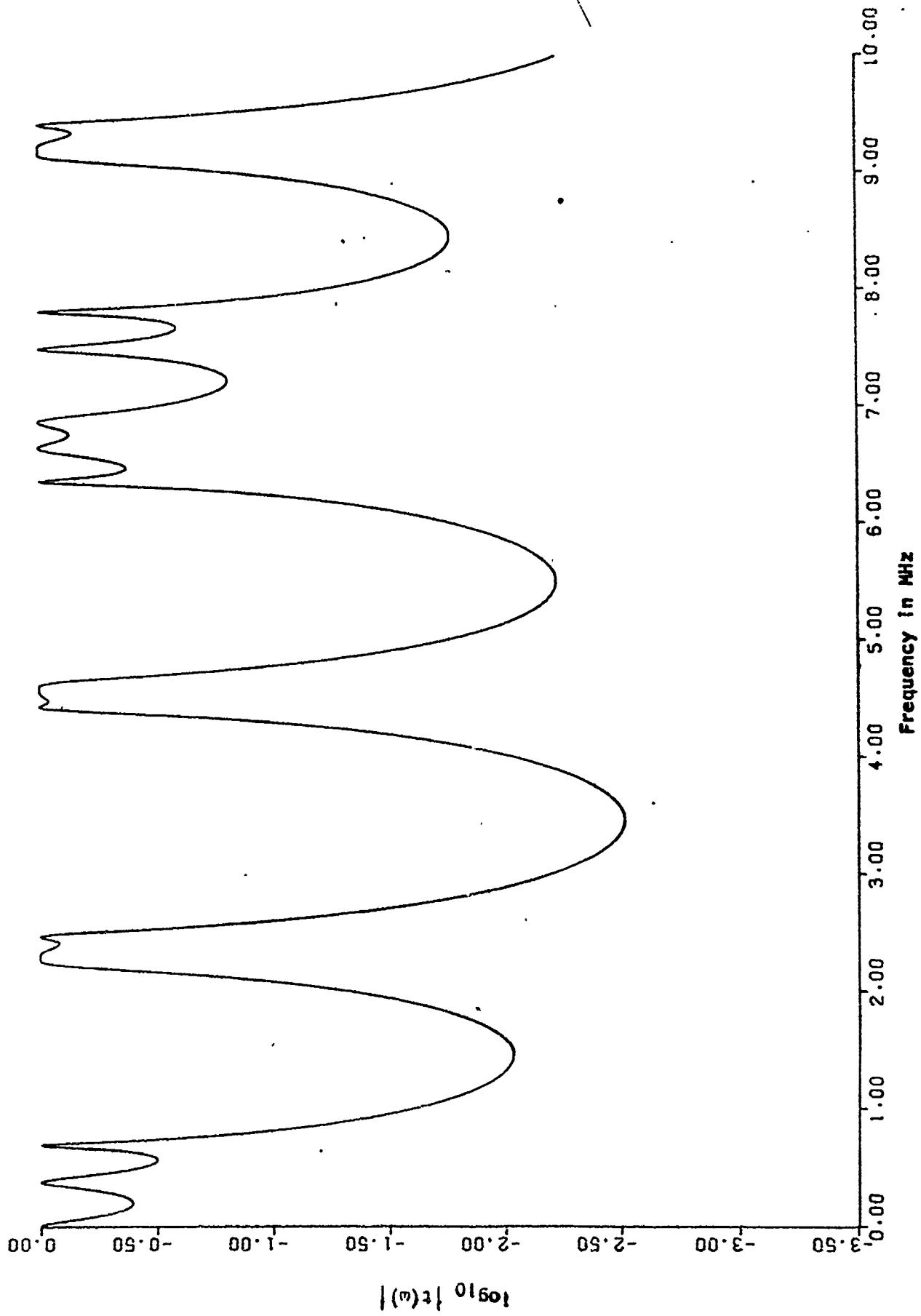


Figure 3e Transmission Spectrum for three 1.22mm Thick Glass Plates in Water

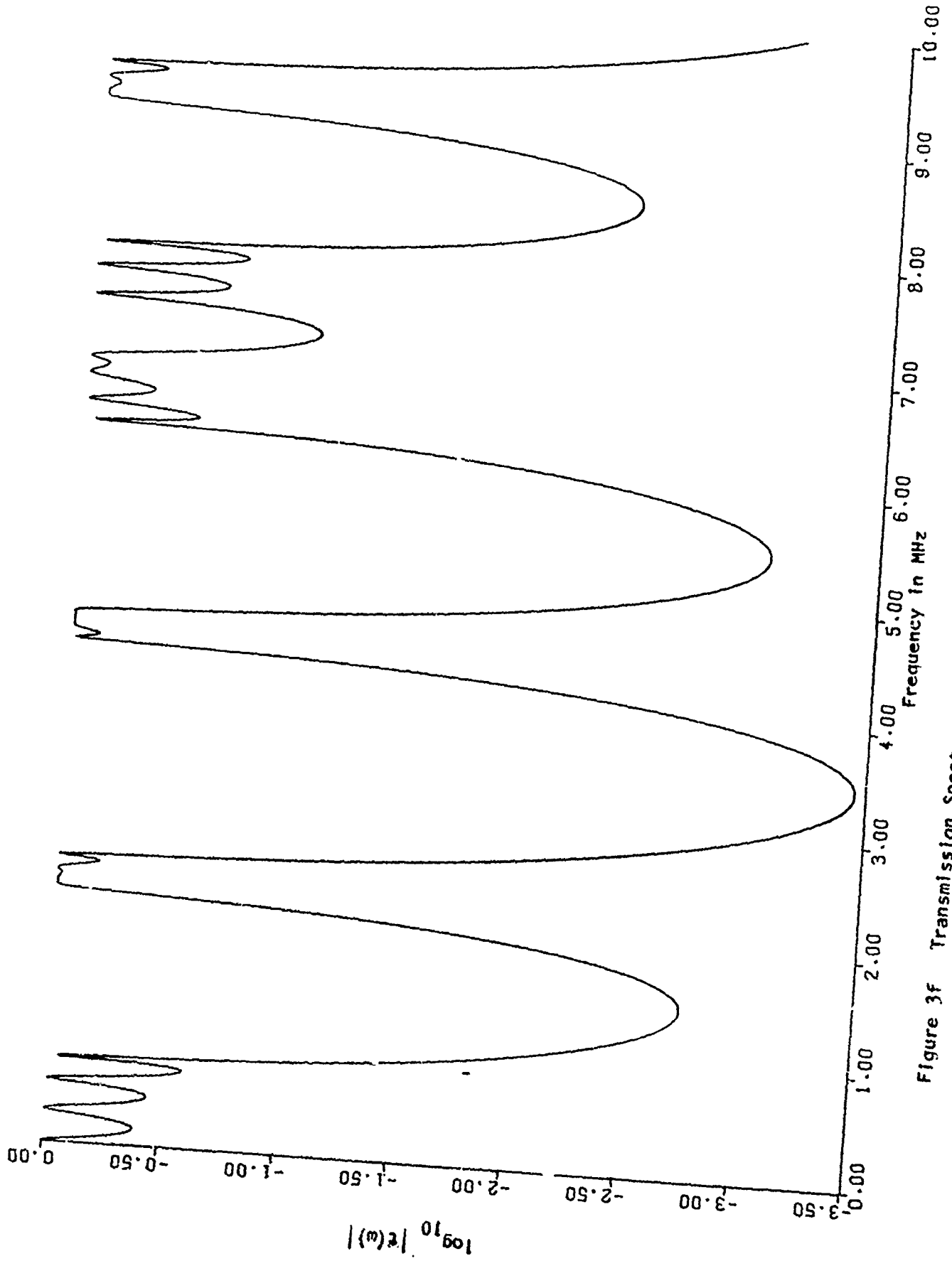


Figure 3f Transmission Spectrum for four 1.22mm Thick Glass Plates in Water

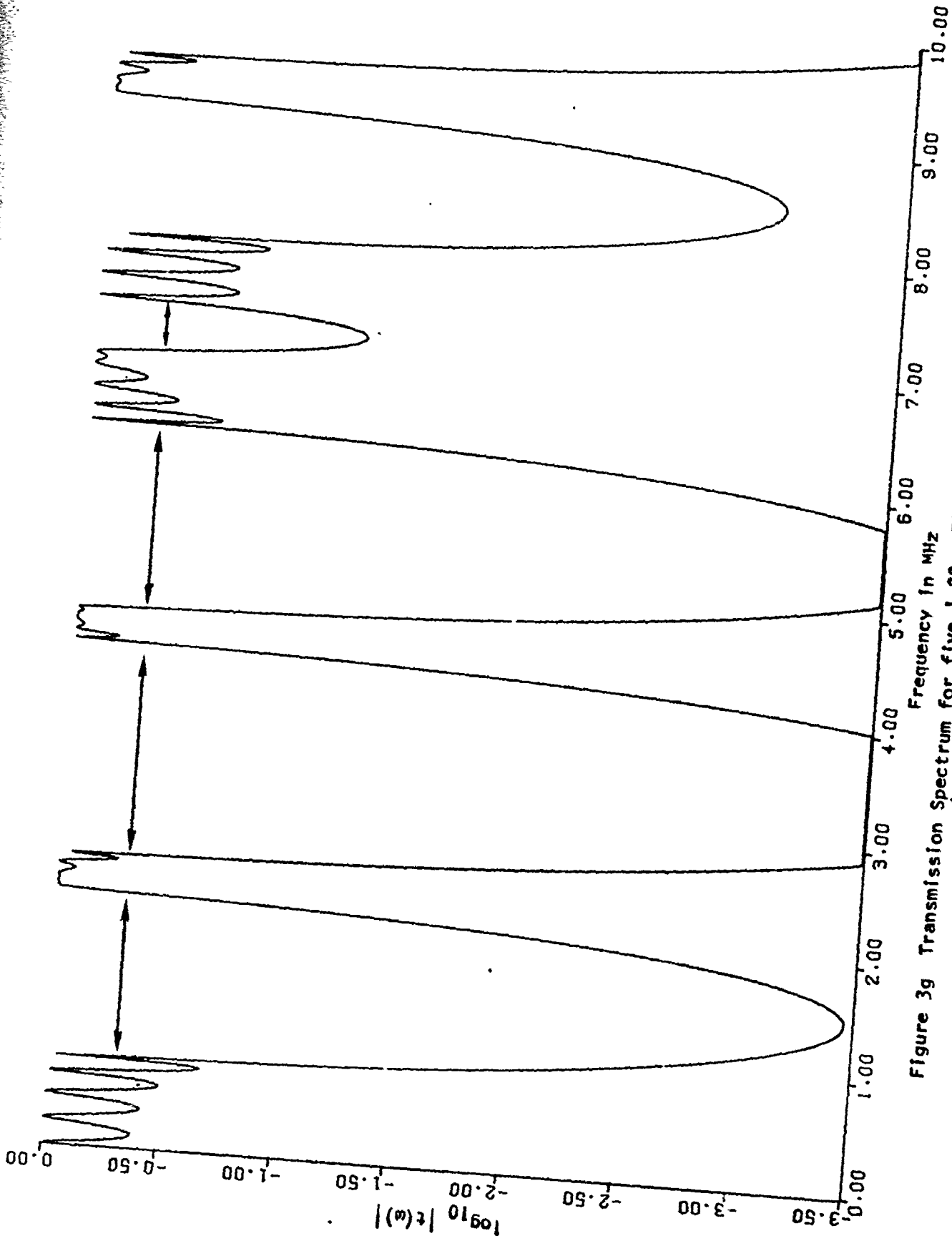


Figure 3g Transmission Spectrum for five 1.22mm Thick Glass Plates in Water
(Arrows denote forbidden bands)

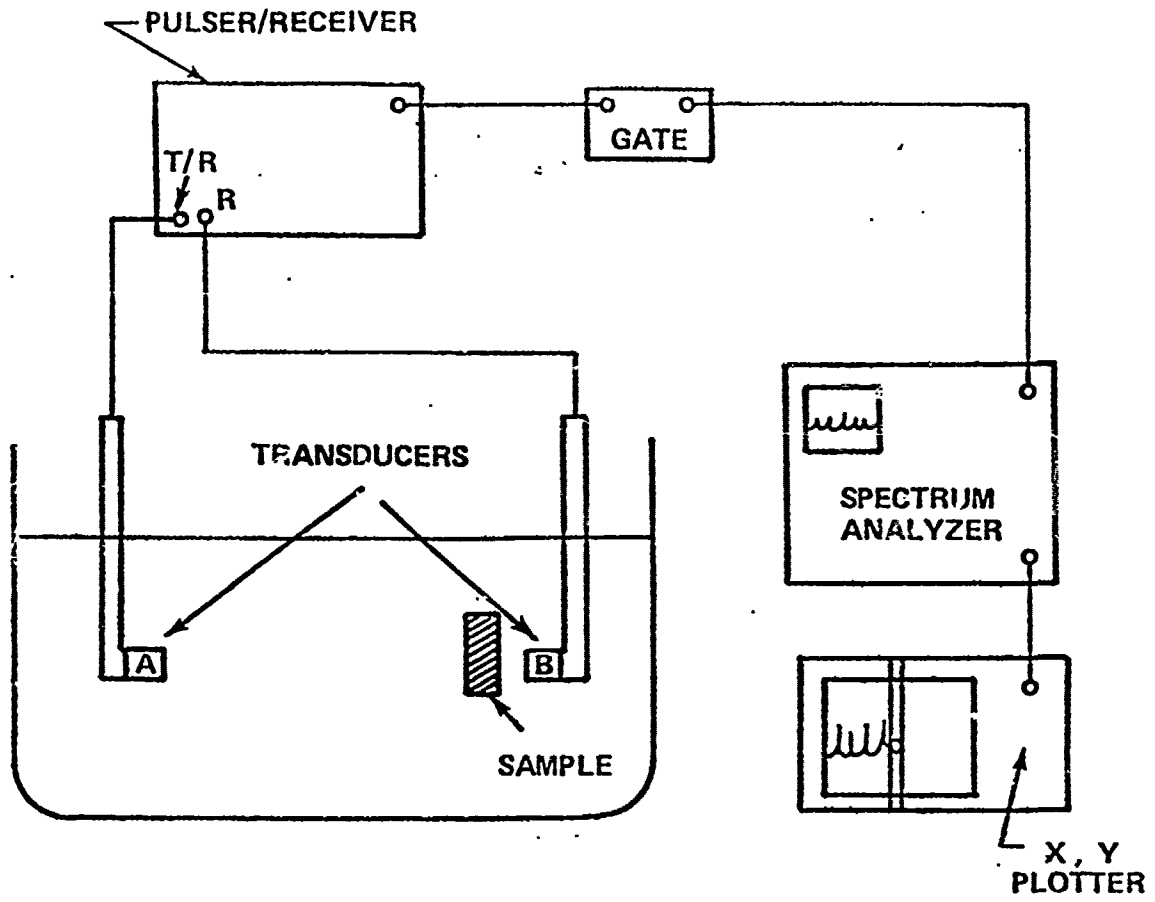


Figure 4 Apparatus for Measuring Acoustic Reflection and Transmission Coefficients as a Function of Frequency

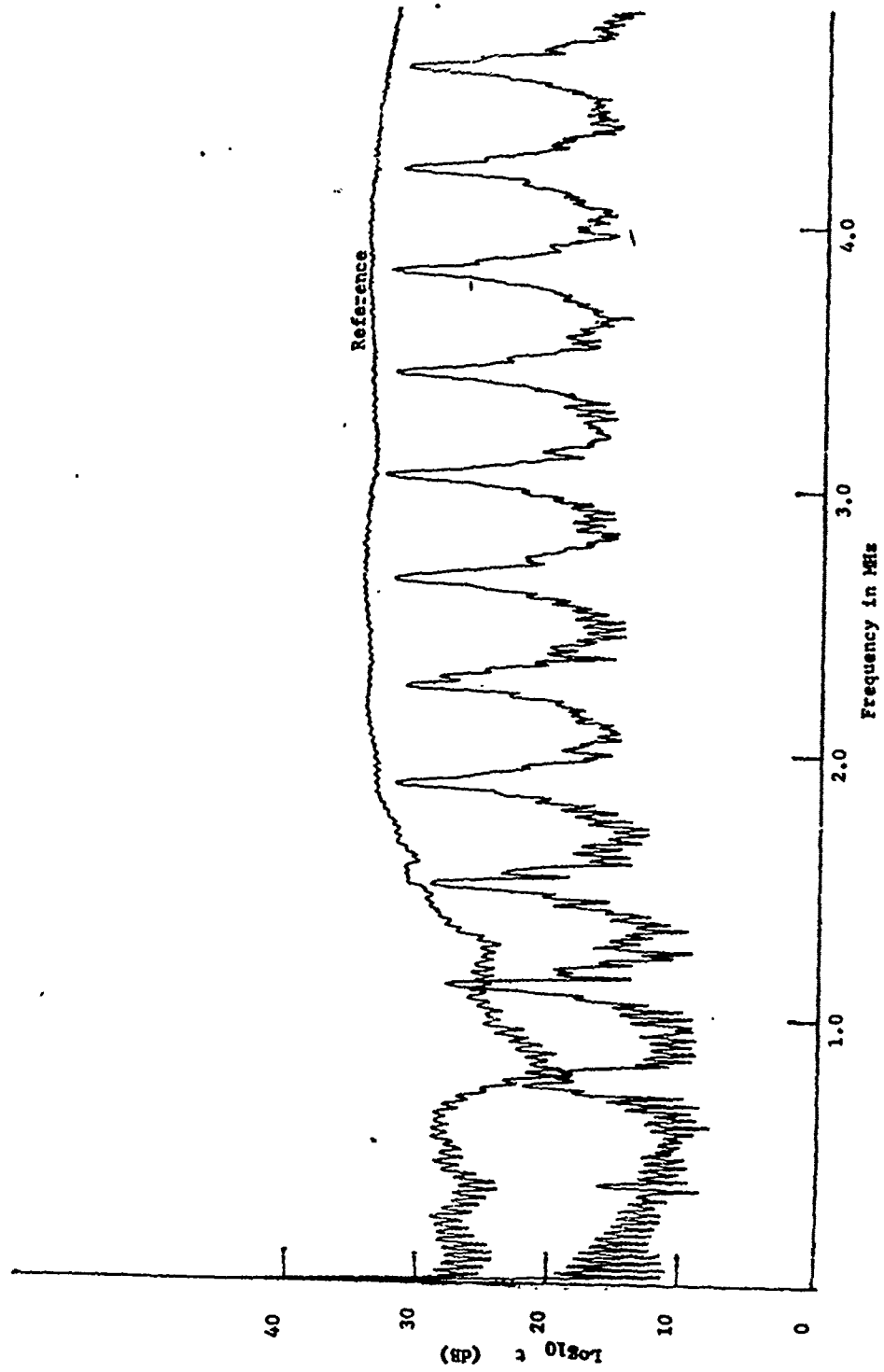


Figure 5 Frequency Dependent Transmission of a .30" Steel Plate

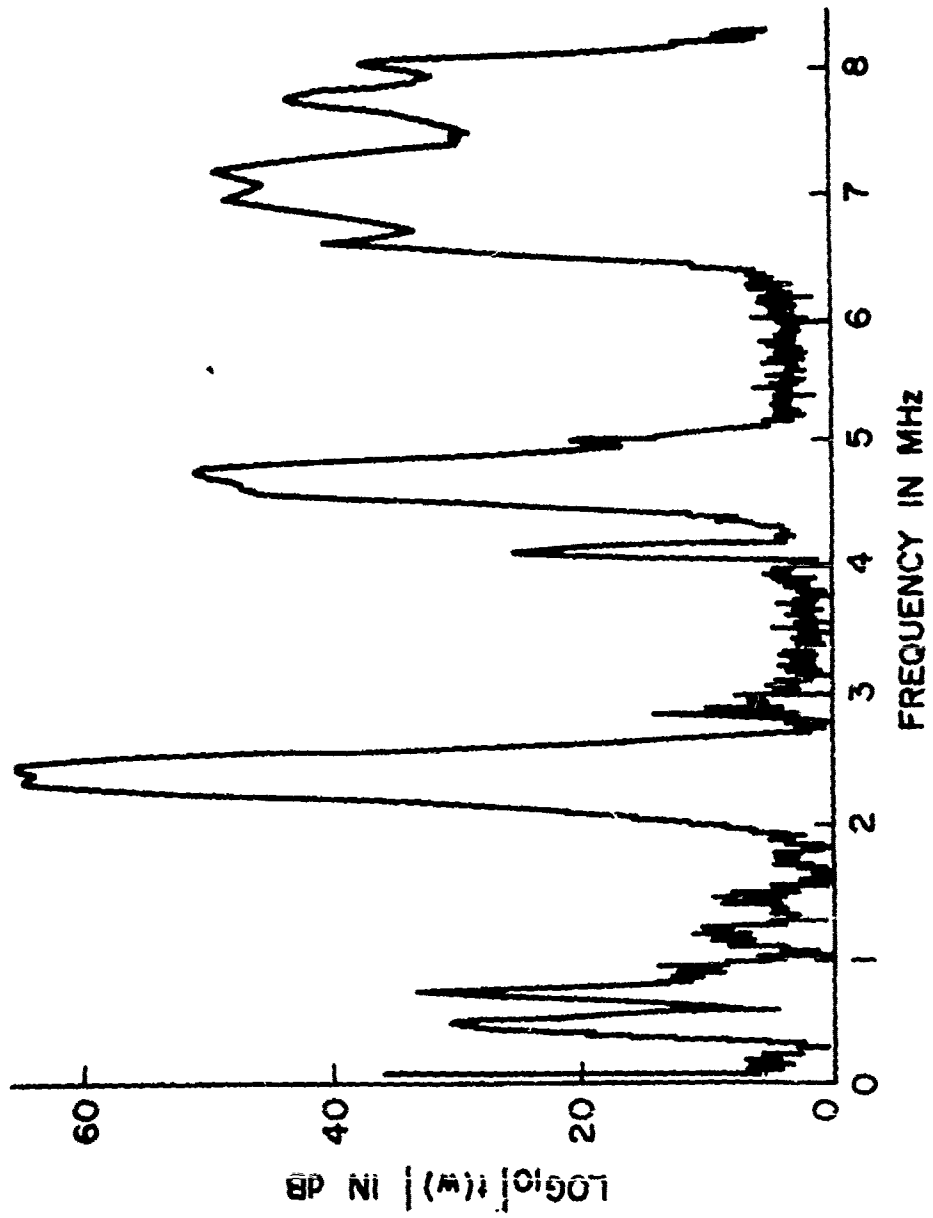


Figure 6. Transmission Spectrum from Layered Array of Three Glass Plates (Measured Experimentally)

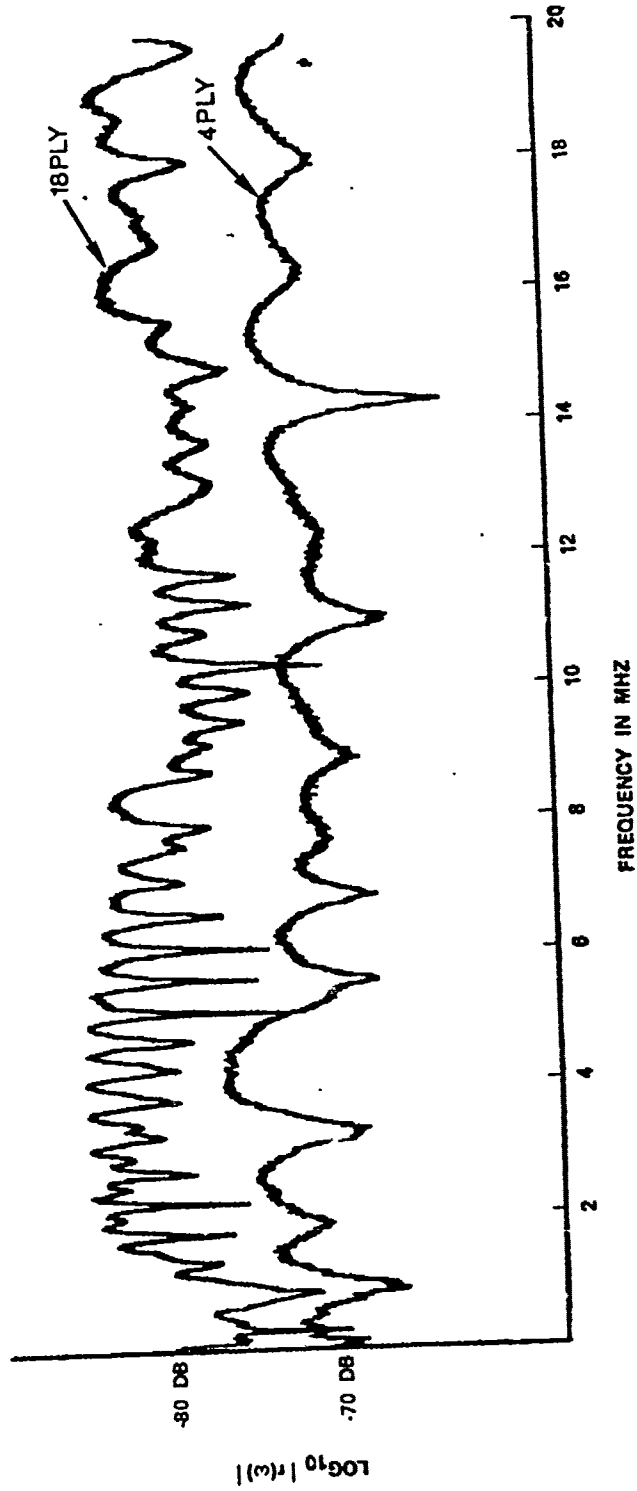


Figure 7 Ultrasonic Frequency Spectra of Graphite Epoxy Panels

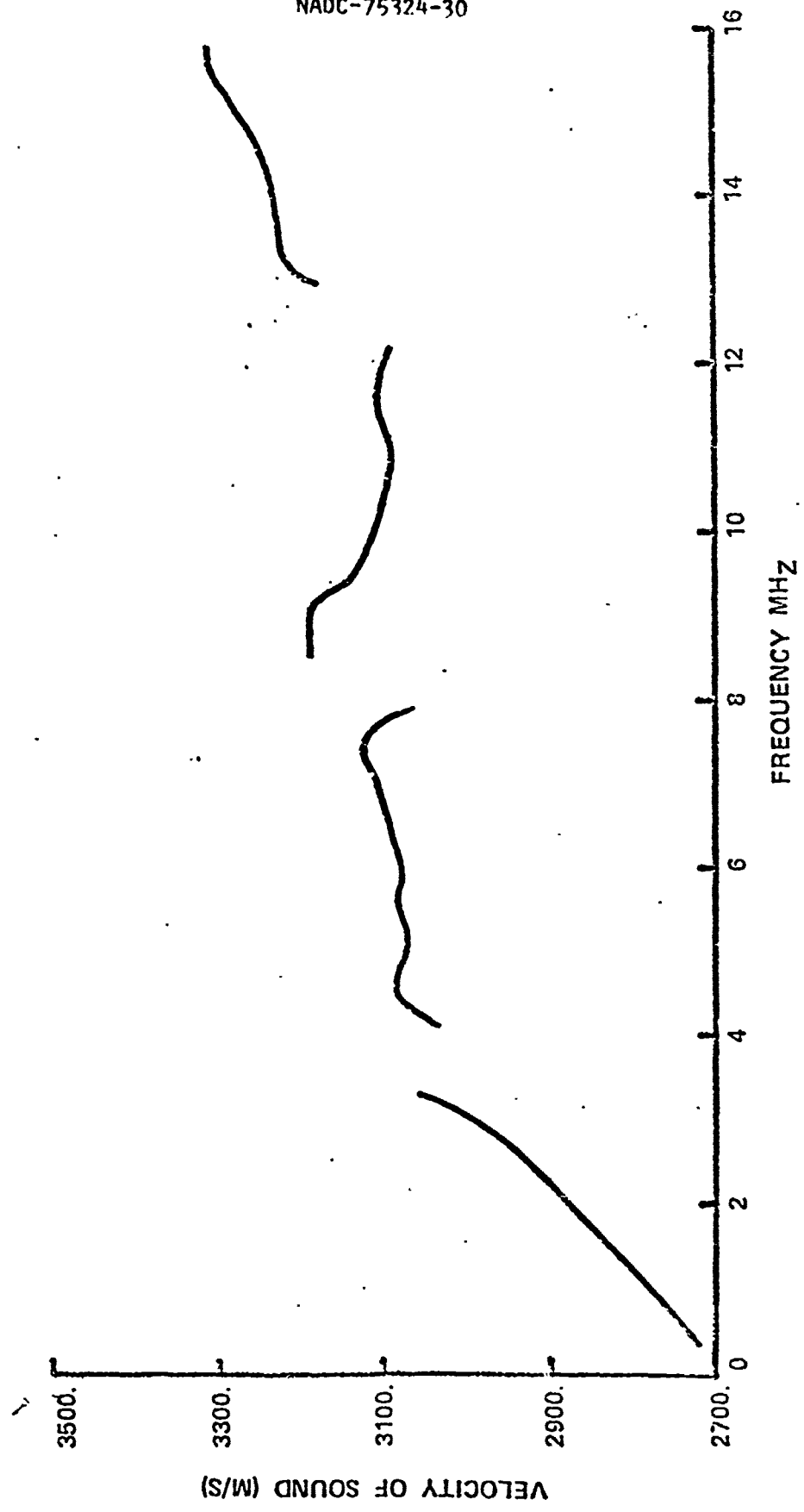


Figure 8 Ultrasonic Velocity vs Frequency in Graphite Epoxy

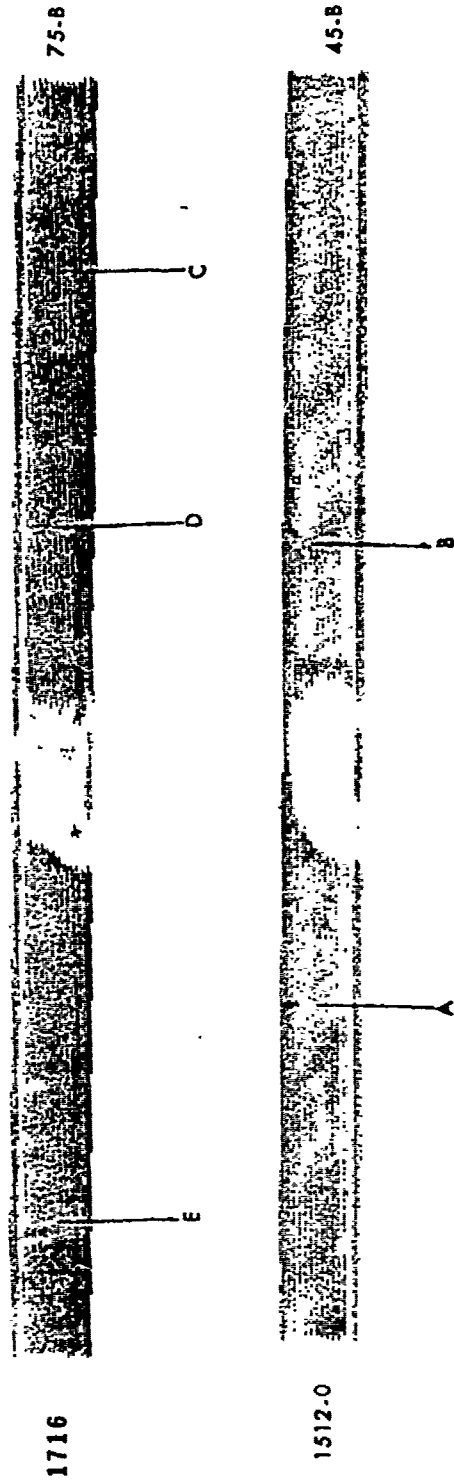


Figure 9 C-Scan of Boron Aluminum Specimens

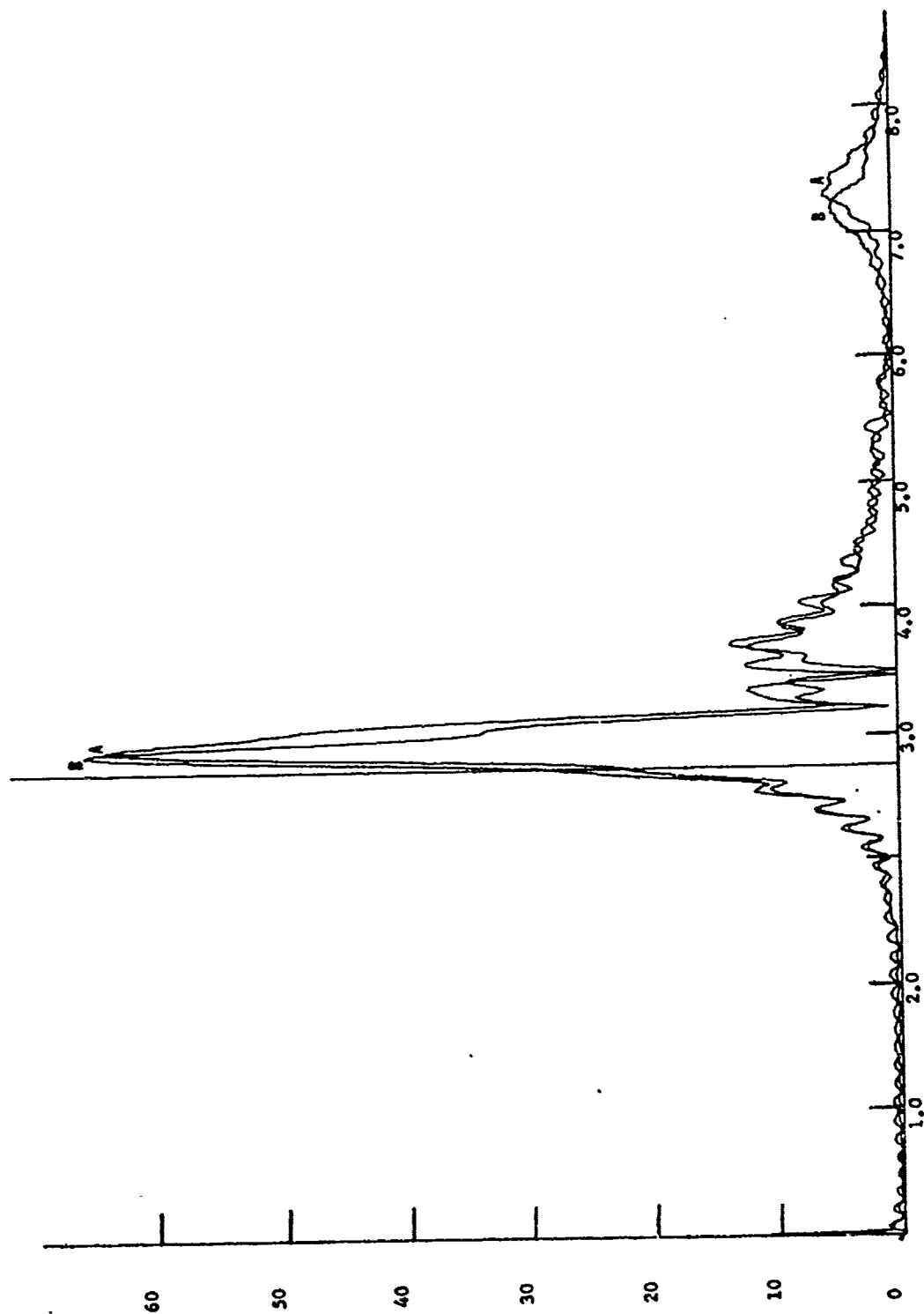


Figure 10a Ultrasonic Frequency Spectra for Boron Aluminum
(letters refer to Figure 9)

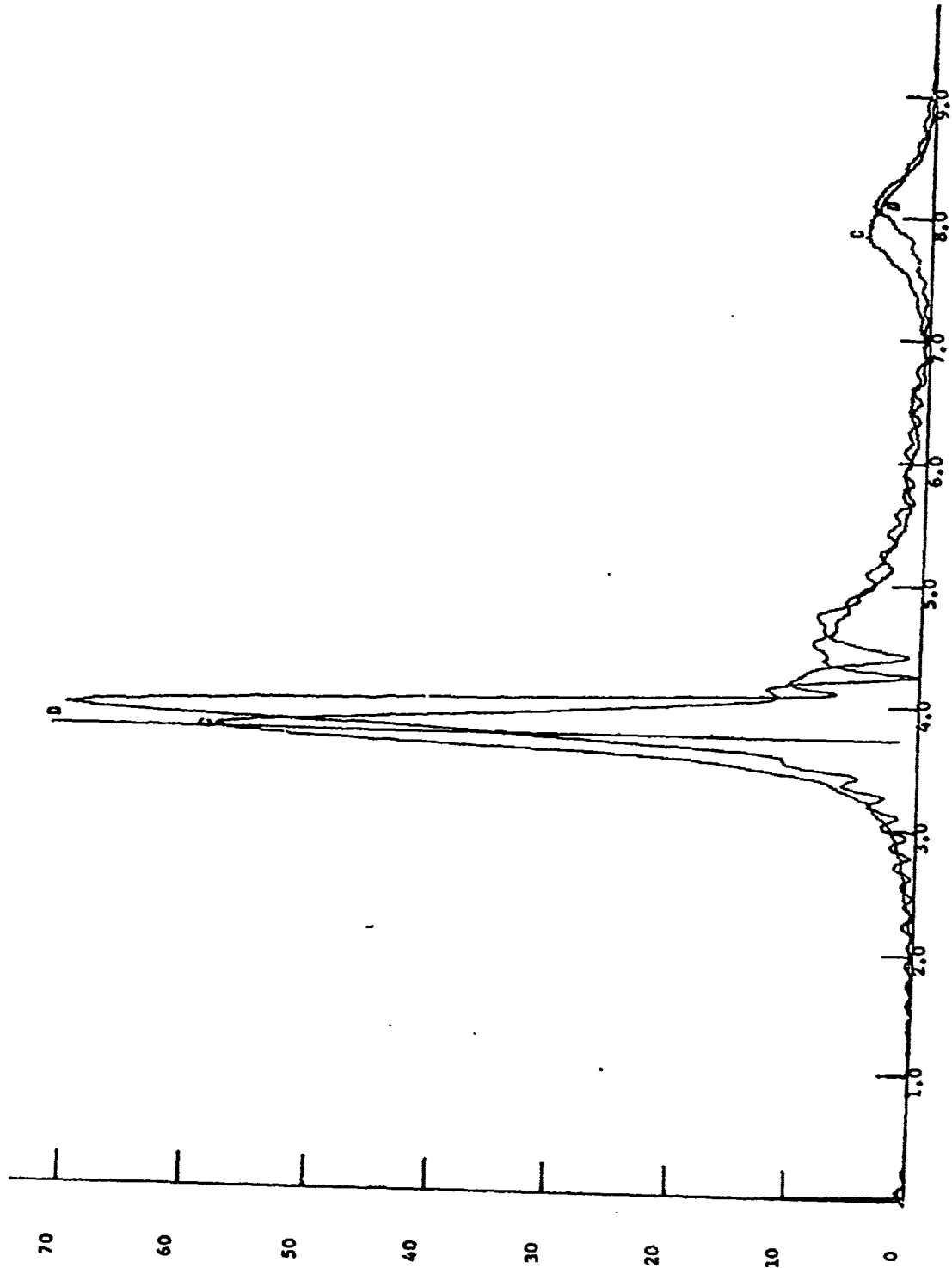


Figure 10b Ultrasonic Frequency Spectra for Boron Aluminum
(letters refer to Figure 9)

NADC-75324-30

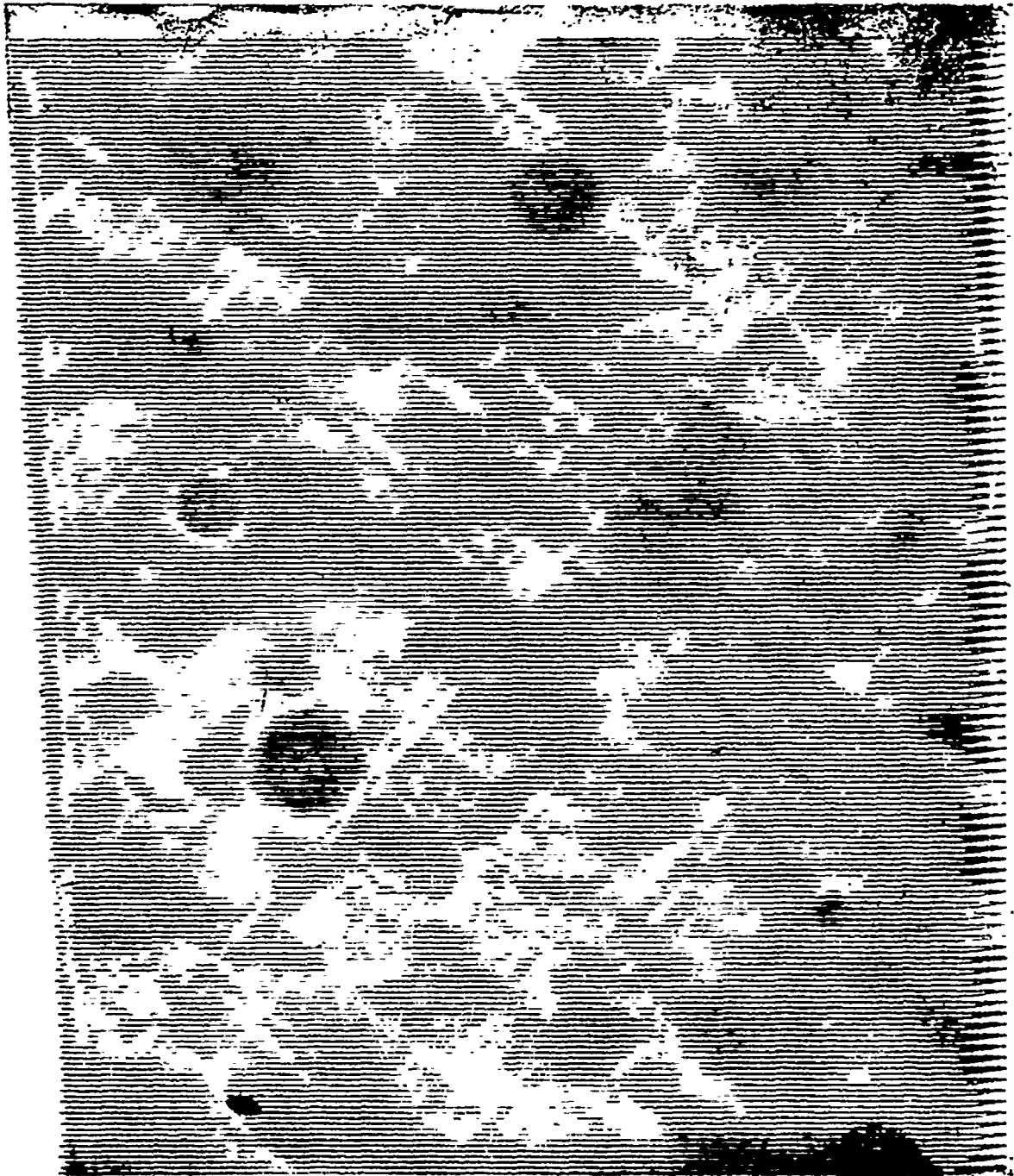


Figure 11 C-scan for Graphite Epoxy Panel Showing
Natural and Synthetic Flaws

R E F E R E N C E S

- (1) J. E. Zimmer, Determination of the Elastic Constants of a Fiber Composite Using Ultrasonic Velocity Measurements, McDonnell Douglas Paper 10181, June 1969
- (2) C. W. Robinson, G. W. Leppelmeier, Experimental Verification of Dispersion Relations for Layered Composites, Journal of Applied Mechanics March 1974, pp 89-91
- (3) Subrata Mukherjee and Erastus H. Lee, Dispersion Relations and Mode Shapes for Waves in Laminated Viscoelastic Composites by Finite Difference Methods, Stanford University Department of Applied Mechanics Report No. 74-7, September 1974
- (4) F. H. Chang, G. W. Yee, J. C. Couchman, Spectral Analysis Technique of Ultrasonic NDT of Advanced Composite Materials, Nondestructive Testing, August 1974, pp 194-198
- (5) J. L. Rose, P. A. Meyer Ultrasonic Procedures for Predicting Adhesive Bond Strength, Materials Evaluation, June 1973
- (6) W. A. Simpson Jr, Time Frequency-Domain Formulation of Ultrasonic Frequency Analysis, Journal of Acoustical Society of America Vol 56, No. 6 December 1974, pp 1776-1781
- (7) L. E. Kinsler and A. R. Frey, Fundamentals of Acoustics Wiley 1962, pp 128-132

D I S T R I B U T I O N L I S T

REPORT NO. NADC-75324-30

AIRTASK R02201001

WORK UNIT DG204

| | <u>No. of Copies</u> |
|--|----------------------|
| NAVAIR (AIR-95A) | 12 |
| (2 for retention) | |
| (1 for AIR-320) | |
| (1 for AIR-4117) | |
| (1 for AIR-4117B) | |
| (1 for AIR-5203) | |
| (1 for AIR-52031) | |
| (1 for AIR-52031B) | |
| (1 for AIR-52031C) | |
| (1 for AIR-52031D) | |
| (1 for AIR-52032) | |
| (1 for AIR-52032D) | |
| WPAFB, Ohio AFML/LA, AFML/LL | 2 |
| DDC | 12 |
| NAVAIRDEVGEN, Warminster, PA. 18974 | 44 |
| (3 for 813) | (1 for 30P6) |
| (2 for 30023) | (1 for 30P7) |
| (1 for 03) | (1 for 301) |
| (1 for 20) | (1 for 302) |
| (1 for 30) | (1 for 303) |
| (1 for 40) | (1 for 304) |
| (1 for 50) | (1 for 305) |
| (1 for 60) | (10 for 3023) |
| (1 for 30P4) | (15 for 30233) |